Repression of pattern-triggered immune responses by hypoxia

Brian C. Mooney[1,2,#], Catherine M. Doorly[1,3,#], Melissa Mantz[4,5], Pablo García[1], Pitter F. Huesgen[4,5,6,7] and Emmanuelle Graciet[1,3*]

[1] Department of Biology, Maynooth University, Maynooth, County Kildare, Ireland

[2] Present address: Department of Biology, University of Oxford, Oxford, UK

[3] Kathleen Lonsdale Institute for Human Health Research, Maynooth University, Maynooth, Co. Kildare, Ireland

[4] Central Institute for Engineering, Electronics and Analytics, ZEA-3, Forschungszentrum Jülich, 52428 Jülich, Germany.

[5] CECAD, Medical Faculty and University Hospital, University of Cologne, 50931 Cologne, Germany

[6] Faculty of Biology, University of Freiburg, Freiburg, Germany

[7] CIBSS- Centre for Integrative Biological Signalling Studies, University of Freiburg, Freiburg, Germany

[#] Equal contribution

[*]Corresponding author: Emmanuelle.Graciet@mu.ie

Keywords: pattern-triggered immunity, hypoxia, stress combination, ERF-VII, N-degron pathway,

Abstract

Biotic and abiotic stresses frequently co-occur in nature, yet, relatively little is known about how plants co-ordinate the response to combined stresses. Previous research has shown that protein degradation by the ubiquitin/proteasome system is central to the regulation of multiple independent stress response pathways in plants. The Arg/N-degron pathway is a subset of the ubiquitin/proteasome system that targets proteins based on their N-termini and has been specifically implicated in the responses to biotic and abiotic stresses including hypoxia *via* degradation of ERF-VII transcription factors, which orchestrate the onset of the hypoxia response program. Here, we investigated the role of the Arg/N-degron pathway in mediating the crosstalk between coinciding abiotic and biotic stresses using hypoxia treatments and the flg22 elicitor of pattern-triggered immunity (PTI), respectively. We uncovered a link between the transcriptional responses of plants to hypoxia and flg22. Combined hypoxia/flg22 treatments showed that hypoxia represses the flg22 transcriptional program, as well as the expression of pattern recognition receptors, MAPK signalling and callose deposition during PTI, through mechanisms that are mostly independent from the ERF-VIIs. These findings aid understanding of the trade-offs between plant responses to combined abiotic/biotic stresses in the context of our efforts to increase crop resilience to global climate change. Our results also show that the well-known repressive effect of hypoxia on innate immunity in animals also applies to plants.

Significance statement

Understanding how plants regulate the crosstalk between stress response pathways is key to our efforts to increase crop resilience and mitigate yield losses caused by global climate change. Despite the urgency to do so, relatively little remains known about how plants respond to combined stresses, which frequently occur in nature. Here, we show that the hypoxia response program and the basal layer of plant immunity (pattern-triggered immunity or PTI) share components. Our data also show that hypoxia represses several key aspects of PTI, a situation akin to that discovered in animals decades ago. These findings have implications for our ability to develop resilient crops by limiting the negative trade-offs that exist between hypoxia response and immunity.

Introduction

A key question in biology is 'how do organisms perceive and respond to environmental cues, as well as stresses?'. While much has been learned about plant responses to individual cues and stresses, the question of how plants integrate information from multiple, combined, stresses to trigger a coordinated response has come to the forefront due to the negative impact of global climate change on crop yields. Studies have shown that the transcriptional response programs to combined stresses can differ considerably from those of the respective individual stresses (Rasmussen et al., 2013; Suzuki et al., 2014; Tan et al., 2023). However, relatively little is known about the mechanisms underpinning such differential transcriptional outputs. The ubiquitin/proteasome system is a key player in coordinating the crosstalk between stress response pathways (reviewed in (Sadanandom et al., 2012; Stone, 2014; Miricescu et al., 2018)) by regulating, for example, the stability of transcriptional regulators that coordinate the crosstalk between phytohormone signalling pathways, such as ethylene/jasmonic acid or jasmonic acid/salicylic acid signalling (Pauwels et al., 2015; Nagels Durand et al., 2016; Miricescu et al., 2018; Wang et al., 2022). The N-degron pathways are a subset of the ubiquitin/proteasome system that target substrate proteins for degradation based on their N-termini (reviewed in (Dissmeyer, 2019; Varshavsky, 2019)). These pathways have been specifically implicated in the responses to a wide range of biotic and abiotic stresses (de Marchi et al., 2016; Gravot et al., 2016; Vicente et al., 2017; Miricescu et al., 2018; Till et al., 2019; Vicente et al., 2019). However, their roles (and that of their substrates) in the regulation of the crosstalk between abiotic/biotic stress response pathways have not been examined.

The arginylation-dependent Arg/N-degron pathway requires the sequential activity of several enzymatic components to modify the N-terminus of substrate proteins before degradation (Fig. 1A). As some of these components are oxygen-dependent, the pathway functions as a *de facto* oxygen sensor that suppresses hypoxia responses in oxygenated conditions *via* the turnover of group VII ETHYLENE RESPONSE FACTOR (ERF-VII) transcription factors, which act as master regulators of the hypoxia response program (Mustroph et al., 2009; Gibbs et al., 2011; Licausi et al., 2011; Reynoso et al., 2019). Other transcriptional regulators, such as LITTLE ZIPPER 2 (ZPR2) and VERNALIZATION2 (VRN2), are also targeted for degradation by the Arg/N-degron pathway in an oxygen-dependent manner (Gibbs et al.,

90 2018; Weits et al., 2019; Labandera et al., 2020). In the case of ERF-VIIs (as well as ZPR2 and
91 VRN2), the N-terminal cysteine (Cys) residue of the proteins is oxidized by PLANT CYSTEINE
92 OXIDASE enzymes (PCOs) (Weits et al., 2014; White et al., 2017; White et al., 2020),
93 followed by the conjugation of arginine (Arg) to their N-terminus by so-called Arg-
94 transferases (ATE1 and ATE2 in *Arabidopsis thaliana*) (Graciet et al., 2009; Zubrycka et al.,
95 2023). This N-terminal Arg (a destabilizing residue) is an N-degron that can be recognized by
96 the PROTEOLYSIS6 (PRT6) E3 ubiquitin ligase, resulting in the degradation of the target
97 proteins (Garzon et al., 2007; Dissmeyer, 2019; Holdsworth et al., 2020; Zubrycka et al.,
98 2023). Arabidopsis *ate1 ate2* (noted *a1a2*) and *prt6* mutants accumulate the ERF-VII
99 transcription factors and consequently display a constitutive activation of the hypoxia
100 response program (Gibbs et al., 2011).
101 The Arg/N-degron pathway has also been implicated in the response of plants to
102 biotic stresses, with varying susceptibility/resistance phenotypes (de Marchi et al., 2016;
103 Gravot et al., 2016; Till et al., 2019; Vicente et al., 2019). The *a1a2* and *prt6* mutants were
104 found to be more susceptible to clubroot gall caused by the biotrophic protist pathogen
105 *Plasmodiophora brassicae* and this susceptibility was dependent on the accumulation of the
106 ERF-VIIs in the Arg/N-degron pathway mutant backgrounds (Gravot et al., 2016).
107 Alternatively, overexpression of some ERF-VIIs correlates with increased resistance to the
108 necrotrophic fungus *Botrytis cinerea* (Zhao et al., 2012). This points to a potential double
109 role of ERF-VIIs in the regulation of hypoxia response and plant defenses against pathogens,
110 but their role in plant innate immune pathways or in the crosstalk between hypoxia
111 response and plant immunity have not been explored in detail.
112 Considering that Arg/N-degron pathway mutants display altered defenses against a
113 range of pathogens with different lifestyles, one hypothesis is that a core aspect of the plant
114 innate immune response, such as pattern-triggered immunity (PTI), is mis-regulated in these
115 mutants. The onset of PTI relies on the detection of conserved Pathogen-Associated
116 Molecular Patterns (PAMPs) at the cell-surface by Pattern Recognition Receptors (PRRs) and
117 triggers a transcriptional reprogramming to activate defense-related genes. Here, using
118 flg22 (derived from bacterial flagellin) as a model PAMP and elicitor of PTI, we sought to
119 determine if (i) the Arg/N-degron pathway contributes to the regulation of PTI; (ii) ERF-VIIs
120 play a role in PTI; and (iii) there is a crosstalk between plant responses to hypoxia and to
121 flg22, which could be regulated by the ERF-VIIs. Our transcriptomic analyses of *a1a2* and

122 wild-type seedlings in response to flg22 treatment suggested a link between hypoxia
123 response and PTI. The use of combined hypoxia/flg22 treatments further showed that
124 hypoxia represses flg22 transcriptional responses, as well as multiple aspects of PTI, such as
125 MAPK signalling and callose deposition, through mechanisms that are largely independent
126 from the ERF-VIIs. In sum, our data reveal that simultaneous exposure to hypoxia and flg22
127 has a repressive effect on PTI, which is analogous to the repression of innate immunity by
128 hypoxia in macrophages (Taylor and Colgan, 2017). This finding is also of relevance to the
129 trade-offs between plant responses to abiotic and biotic stresses in our efforts to increase
130 crop resilience to mitigate the yield losses caused by global climate change.
131

132 ## Results

133 **Transcriptomic response of *a1a2* seedlings to flg22**

134 To explore whether the Arg/N-degron pathway plays a role in the regulation of PTI, we first
135 used RNA-sequencing (RNA-seq) to compare the genome-wide expression changes of *a1a2*
136 and wild-type seedlings treated with 1 µM flg22 for 1 hr (Fig. S1A). When comparing flg22 to
137 mock-treated seedlings (flg/m), the total number of differentially expressed genes (DEGs;
138 adj. *p*-value<0.05 and $|\log_2(FC)|>0.585$) was similar in wild-type (Col-0) and in *a1a2*
139 seedlings (~4,400 DEGs), as well as the number of up- and down-regulated genes (~2,800
140 up-regulated and ~ 1,500 down-regulated genes) (Fig. 1B). Our two datasets had a large
141 overlap with a previously published transcriptomic dataset obtained under similar
142 experimental conditions (Fig. S1B). PTI-associated Gene Ontology (GO) terms were over-
143 represented among the DEGs in wild-type and in *a1a2* seedlings after flg22 treatment (*e.g.*
144 'innate immune response', 'response to salicylic acid stimulus', 'callose deposition in cell
145 wall', 'MAPKKK cascade', or 'response to oxidative stress') (Fig. S1C and Supplemental
146 Dataset 1). Differences in the flg22 transcriptional response of the *a1a2* mutant compared
147 to the wild type were also found, with 700 and 507 DEGs being specific to either *a1a2* or the
148 wild type, respectively (Fig. S1B). We also tested whether there were differences in the
149 amplitude of gene expression changes in DEGs that were common to the two genotypes,
150 and found that in response to flg22, the directionality and amplitude of gene expression
151 changes were comparable in *a1a2* and Col-0 (Fig. S1I).

152 For a more stringent comparison between *a1a2* and wild-type seedlings, we re-
153 analyzed the RNA-seq data by comparing directly the two genotypes under either mock
154 (a1a2/Col-0 (m)) or flg22 treatment (a1a2/Col-0 (flg)) (cut-offs applied: adj. *p*-value<0.05
155 and $|\log_2(FC)|>0.585$). This analysis revealed 104 DEGs in a1a2/Col-0 (m) and 97 DEGs for
156 a1a2/Col-0 (flg) (Fig. 1C). A GO analysis of all DEGs in *a1a2 versus* wild-type seedlings
157 retrieved GO categories related to known functions of the Arg/N-degron pathway (Fig. S1D
158 and Supplemental Data 2), including 'response to hypoxia', 'regulation of seed germination',
159 'regulation of lipid metabolic process' and 'glycoside metabolic process' (Holman et al.,
160 2009; Gibbs et al., 2011; Gibbs et al., 2014; de Marchi et al., 2016; Zhang et al., 2018). The
161 directionality of the gene expression changes was also as expected, with the expression of
162 several known hypoxia response genes being constitutively induced in *a1a2* (Fig. S1E). Of
163 the DEGs identified in both a1a2/Col-0 datasets, 59 were differentially expressed in *a1a2*
164 independently of the flg22 treatment (Fig. S1F) and these common DEGs were associated
165 with GO categories known to be constitutively mis-regulated in *a1a2* mutants, such as
166 'protein arginylation' and 'response to hypoxia' (Holman et al., 2009; Gibbs et al., 2011; de
167 Marchi et al., 2016). Relatively few genes (28) were specifically mis-regulated in the *a1a2*
168 mutant in response to flg22 (Fig. S1F). For a subset of these genes, we validated that the
169 transcriptional mis-regulation was dependent on the loss of Arg-transferase activity in *a1a2*
170 by using a rescue line (Graciet et al., 2009) with the ATE1 genomic locus re-introduced to
171 the *a1a2* background (Fig. S1G). Based on the RNA-seq data, the majority of these 28 DEGs
172 had lower expression in *a1a2* compared to the wild type after flg22 treatment (Fig. S1H),
173 with several having known functions in the regulation of plant defenses against pathogens
174 (*e.g. PLANT DEFENSIN2.1* (*PDF2.1*); *VEGETATIVE STORAGE PROTEIN1* (*VSP1*); *CYSTEINE-RICH*
175 *RLK25* (*CRK25*); *CHITINASE A* (*CHIA*)). Six of these genes were expressed at higher levels in
176 *a1a2* compared to the wild type after flg22 treatment.
177 The *a1a2* mutant is expected to accumulate Arg/N-degron pathway substrates,
178 which could result in protein abundance differences without transcriptional changes. We
179 hence also conducted a proteomic comparison of *a1a2* and wild-type seedlings: 74 proteins
180 accumulated differently in at least one of the four comparisons (a1a2 (flg/m); Col-0 (flg/m);
181 a1a2/Col-0 (m) or a1a2/Col-0 (flg); cut-off applied: multi-sample ANOVA with permutation-
182 based FDR< 0.05, followed by Tukey´s *post-hoc* test with FDR<0.05). A comparison of the
183 fold-changes in the proteomic and RNA-seq datasets indicated a strong positive correlation

184 (Pearson r ~ 0.8) (Fig. 1D,E). This included proteins/genes up-regulated by hypoxia response
185 (*e.g.* ADH1 and HB1), and proteins involved in glucosinolate biosynthesis (*e.g.* BCAT4, TGG2,
186 IGMT5), which were found to be less abundant in *a1a2* in agreement with their lower
187 expression (de Marchi et al., 2016). A small number of proteins/genes behaved differently in
188 the mock-treated *a1a2* mutant compared to the wild type, with some having known roles in
189 plant defense (*e.g.* SENESCENCE-ASSOCIATED GENE 21 (SAG21) (Salleh et al., 2012)).
190 Finally, we examined whether the transcriptional differences identified between
191 flg22-treated *a1a2* and wild-type seedlings could be sufficient to affect PTI. We first tested
192 the effect of prolonged flg22 exposure using seedling growth inhibition (Fig. 1F) and root
193 growth inhibition assays (Fig. S1J). Both indicated that the *a1a2* mutant and the wild type
194 were affected in a similar manner by flg22. The production of apoplastic reactive oxygen
195 species (ROS) upon flg22 treatment was also not affected in the *a1a2* mutant compared to
196 the wild type (Fig. S1K). In contrast, callose deposition assays showed that *a1a2* was
197 negatively affected for callose deposition in response to flg22 treatment (Fig. 1G). This could
198 be a consequence of (i) reduced up-regulation of *GLUCAN SYNTHASE-LIKE5* (*GSL5*), an
199 important callose synthase during flg22 response (Luna et al., 2011), in *a1a2* seedlings
200 ($\log_2$(flg/m)=0.815) compared to the wild-type ($\log_2$(flg/m)=1.023); or (ii) *a1a2* having lower
201 levels of glucosinolates (de Marchi et al., 2016), which are important for callose biosynthesis
202 (Clay et al., 2009). Alternatively, the constitutive activation of hypoxia response in *a1a2*
203 could also contribute to the decreased callose deposition phenotype (*e.g.* callose content
204 changes upon hypoxia treatment of wheat seedlings (Subbaiah and Sachs, 2001; Albrecht
205 and Mustroph, 2003)).
206
207 **Hypoxia and flg22 transcriptional response programs overlap**
208 Our data suggest a potential connection between hypoxia and flg22 responses and our RNA-
209 seq analysis also revealed that genes associated with the GO categories 'response to oxygen
210 levels' and 'response to hypoxia' were enriched among flg22-responsive genes in the wild
211 type (Col-0 flg/m) and in *a1a2* (a1a2 flg/m) (Fig. 2A and Supplemental Dataset 1). We
212 carried out a similar GO analysis using (i) the Arabidopsis flg22 response dataset from
213 Denoux *et al*. (Denoux et al., 2008); and (ii) a dataset composed of conserved flg22-
214 responsive genes in 4 different species of Brassicaceae (termed 'Brassicaceae core PTI')
215 (Winkelmuller et al., 2021). A similar enrichment for the 'response to hypoxia' and 'response

216 to oxygen levels' was found (Fig. 2A), with several hypoxia-related DEGs common to at least
217 two datasets showing the same directionality of expression changes (Fig. S2A). In our Col-0
218 flg/m dataset, DEGs found in these GO categories included *ERF73/HRE1* (AT1G72360),
219 *ERF71/HRE2* (AT2G47520; Fig. S1E), *HEMOGLOBIN1* (*HB1*; AT2G16060; Fig. S1E) or *Alanine*
220 *AMINOTRANSFERASE1* (*AlaAT1*; AT2G47520), as well as *ENHANCED DISEASE SUSCEPTIBILITY*
221 *1* (*EDS1*) and *PHYTOALEXIN DEFICIENT 4* (*PAD4*).
222 The overlap between the transcriptional responses to flg22 and to hypoxia was
223 further explored by comparing our Col-0 flg/m dataset with a list of hypoxia responsive
224 genes in 7-day old Arabidopsis seedlings treated with 2 hrs of hypoxia ($O_2 < 2\%$) compared
225 to normoxia ($|\log_2(FC)|>1.0$ and FDR<0.05) (Lee and Bailey-Serres, 2019)). This analysis
226 revealed a statistically significant overlap (p-value<10^{-4}; Chi square test) of 384 DEGs (Fig. 2B
227 and Fig. S3). The majority of these common DEGs had the same directionality of gene
228 expression change in response to hypoxia and to flg22 (Fig. 2C). This was the case for typical
229 flg22 response genes (*e.g. WRKY33* or *CPK28*), hypoxia response genes (*e.g. LBD41* or *HRE2*),
230 or genes known to be involved in both response pathways (*e.g. RBOHD, MPK3* or *HB1*). One
231 notable exception was *FLS2*, which codes for the flg22 PRR, and whose transcription was
232 repressed under hypoxia, while being up-regulated upon flg22 treatment. GO analysis of the
233 384 common DEGs indicated an enrichment for genes associated with defense-related
234 processes (*e.g.* 'defense response by callose deposition', 'indole glucosinolate metabolic
235 process' or 'defense response') and the response to oxygen levels (Supplemental Dataset 4).
236 There was also an over-representation of response genes to other abiotic stresses (*e.g.*
237 osmotic stress, temperature), and to stress-related hormone signalling pathways (*i.e.*
238 ethylene, salicylic acid and jasmonic acid).
239 To determine if the overlap of hypoxia and flg22 responses could be a conserved
240 feature of the flg22 transcriptional response program, we also compared the Brassicaceae
241 core PTI dataset (Winkelmuller et al., 2021) and hypoxia response genes (Lee and Bailey-
242 Serres, 2019). A statistically significant overlap (p-value<10^{-4}; Chi square test) of 118 DEGs
243 was found (Fig. S2B), and similarly to the comparison with our Col-0 flg/m dataset, most
244 common genes had the same directionality of gene expression change (Fig. S2C). Hence, the
245 common regulation of a subset of hypoxia and flg22 response genes appears to be a
246 conserved feature, at least within the Brassicaceae family.

247 Because the ERF-VII transcription factors are the master regulators of the
248 transcriptional response program to hypoxia, we explored whether the common regulation
249 of some genes by both flg22 or hypoxia requires the ERF-VIIs. To this end, the expression of
250 a subset of genes was determined in Col-0 and in an *erfVII* quintuple mutant (Abbas et al.,
251 2015) following mock or flg22 treatment (Fig. 2D). The selected genes were differentially
252 expressed in the 2HS/2NS dataset (Lee and Bailey-Serres, 2019) and in our Col-0 flg/m
253 dataset, and either (i) responded more strongly in a1a2 flg/m compared Col-0 flg/m; or (ii)
254 were already significantly up-regulated in mock-treated a1a2 (likely because of the ERF-VII
255 accumulation). This analysis indicates that the regulation of some hypoxia response genes
256 by flg22 treatment is likely not ERF-VII-dependent.
257
258 **Hypoxia represses the flg22 transcriptional response program**
259 To examine the potential crosstalk between hypoxia and flg22 responses, the genome-wide
260 expression changes that occur under individual (hypoxia or flg22) and combined
261 hypoxia/flg22 treatments were determined in wild-type Col-0 seedlings. We focused on a
262 relatively short 1 hr treatment that enabled monitoring of the onset of both flg22 and
263 hypoxia responses (Fig. S4A). The DEGs (cut-offs: adj. *p*-value<0.05 and $|\log_2(FC)|>0.585$)
264 identified under individual hypoxia (HM v NM; hypoxia/mock v normoxia/mock) or flg22 (NF
265 v NM; normoxia/flg22 v normoxia/mock) treatments compared to untreated seedlings
266 overlapped with those obtained in other similar published datasets (Denoux et al., 2008; Lee
267 and Bailey-Serres, 2019) (Fig. S4B-C), and retrieved an enrichment for expected GO
268 categories (Suppl. Dataset 5). Analysis of the number of DEGs indicated that flg22 treatment
269 alone induced greater transcriptional changes (NF v NM; 1906 DEGs) than hypoxia alone
270 (HM v NM; 145 DEGs), likely because of the short 1 hr treatment (Fig. 3A). Combining
271 hypoxia/flg22 resulted in even larger transcriptional changes (HF v NM; 2612 DEGs) than
272 flg22 treatment alone (Fig. 3A). A comparison of the three datasets showed a large overlap
273 between the responses to flg22 alone (NF v NM) and to combined hypoxia/flg22 treatment
274 (HF v NM; 1601 DEGs in common), and a smaller overlap between hypoxia and combined
275 hypoxia/flg22 treatments (131 DEGs) (Fig. 3B). In addition, 59 genes were commonly
276 differentially expressed in all conditions, with an over-representation of genes associated
277 with metabolic processes (*e.g.* 'response to carbohydrate stimulus'), hormone signalling
278 (ethylene, abscisic acid and brassinosteroids), immunity ('response to chitin') and

279 development (‘root hair elongation’ or ‘developmental maturation’) (Suppl. Dataset 5). The
280 vast majority of these 59 DEGs showed the same directionality of gene expression change
281 irrespective of the stress applied (Fig. S4D). For the 53 genes that were up-regulated in all
282 conditions (Fig. 3C), the combined hypoxia/flg22 treatment enhanced the amplitude of up-
283 regulation (Fig. 3D and 3E). While there were only 2 common genes being down-regulated
284 (Fig. 3F), the same trend was observed, such that combined hypoxia/flg22 resulted in a
285 stronger repression of these 2 genes compared to hypoxia or flg22 alone (Fig. 3G).
286 Strikingly, 939 genes were uniquely regulated in response to combined hypoxia/flg22
287 (HF v NM), indicating that the combined stress elicits a distinct transcriptional response. GO
288 analysis of these 939 hypoxia/flg22-specific DEGs revealed an enrichment for genes
289 associated with expected defense and phosphorylation-related functional GO categories.
290 GO analysis for molecular functions revealed an over-representation of transcription factor-
291 coding genes (Suppl. Dataset 5), with bHLH, Zn finger and homeobox transcription factors
292 accounting for a larger number of differentially expressed transcription factors (Fig. S4E).
293 The expression of these transcription factors was mostly repressed by hypoxia/flg22
294 treatment, while NAC, WRKY and bZIP transcription factors were up-regulated. In contrast,
295 the 304 DEGs specific to flg22 treatment did not have an over-representation of
296 transcription factor coding genes, so this appears to be a unique feature of the response
297 program to combined hypoxia/flg22 (Suppl. Dataset 5). Separate GO analyses for uniquely
298 down-regulated genes upon hypoxia/flg22 revealed an enrichment for terms associated
299 with developmental processes, such as ‘morphogenesis of polarized epithelium’, including
300 genes associated with phytohormone signalling pathways with roles in cell division and
301 differentiation (*i.e.* auxin and cytokinin signalling) (Fig. 3H). In contrast, genes that were
302 uniquely up-regulated after the combined treatment were enriched for genes associated
303 with stress responses (*e.g.* response to heat), suggesting that the response to combined
304 stresses could be broader and overlap with that of other individual stresses (Fig. 3H).
305 To further characterize the crosstalk between hypoxia and flg22 responses, we used
306 three metrics established to study the crosstalk between the transcriptional programs to
307 combined abiotic stresses in *Marchantia polymorpha* (Tan et al., 2023) (see also Fig. S4F for
308 calculations). Specifically, these metrics allow the quantification of (i) shared aspects of the
309 transcriptional response programs (similarity score ranges from 0 to 1, with 1 corresponding
310 to identical response programs), (ii) stress dominance (suppression score varies between -1

311 and 1, with a negative score indicating a suppression of flg22 response by hypoxia), and (iii)
312 novel components of combined treatments (novel interaction score; varies between 0 and
313 1, with 1 indicating that combined stresses results in an entirely new transcriptional
314 program) (Tan et al., 2023). For both up- and down-regulated genes, the negative
315 suppression score obtained suggests that the hypoxia response program represses flg22
316 transcriptional response (Fig. 3I). The lower suppression score obtained for down-regulated
317 genes (-0.16) suggests that the repression of down-regulated genes by hypoxia could be of
318 relevance. The novel interaction scores obtained further indicate that combined
319 hypoxia/flg22 elicits a transcriptional response that is different from each of the individual
320 stresses. The novel interaction score for up-regulated genes (0.241) is in line with the
321 average novel interaction scores for up-regulated genes in response to 18 combined
322 treatments in Marchantia (0.29). Notably, the novel interaction score for down-regulated
323 genes (0.678) is higher than in Marchantia, in which the highest score obtained for down-
324 regulated genes was 0.56 (18 treatments). This indicates that the repression of specific
325 genes under combined hypoxia/flg22 might be a particularly important aspect of the unique
326 response to this combined stress. A GO analysis of the 480 down-regulated genes under
327 hypoxia/flg22 only (Fig. 3H) suggests an over-representation for genes associated with
328 development. Strikingly, there is also an enrichment for genes coding for cytochrome P450
329 enzymes, which use molecular oxygen to catalyze the oxidation of other molecules (Suppl.
330 Dataset 5).
331 The metrics derived from our RNA-seq dataset analysis suggest that hypoxia
332 represses some aspects of flg22 response. We therefore examined more carefully the 304
333 DEGs (Fig. 3B) identified only after flg22 treatment (*i.e*. these genes no longer respond to
334 flg22, when combined with hypoxia). A GO analysis of these DEGs showed an enrichment
335 for molecular functions associated with phosphorylation ('kinase activity'), 'carbohydrate
336 binding' and 'transmembrane receptor protein kinase'. Notably, genes in the latter GO
337 category included PRRs such as *FLS2* and *EFR*. Hence, our data suggest that one particular
338 aspect of the repression of flg22 response by hypoxia could occur at the level of PRR
339 expression.
340
341 **Hypoxia suppresses PTI**

342 Next, we tested whether different aspects of PTI were also repressed by combined
343 hypoxia/flg22, and examined if ERF-VII transcription factors played a role in the repression
344 of PTI under hypoxic conditions. We first used root growth inhibition assays to reveal
345 additive or synergistic effects of the combined treatment (Fig. 4A) because both flg22 and
346 hypoxia suppress root elongation. Either flg22 (NF) or hypoxia (HM) treatments resulted in
347 decreased root elongation compared to the same genotype in control conditions
348 (normoxia/mock (NM)). Combined hypoxia/flg22 (HF) did not enhance the inhibitory effects
349 of hypoxia on root elongation in Col-0. In contrast, the *erfVII* quintuple mutant was more
350 severely affected by the combined stress compared to HM and NF conditions, thus
351 suggesting that ERF-VIIs in the wild type may contribute to protecting the root meristem
352 under combined hypoxia/flg22 treatment. Expression analysis by RT-qPCR of selected
353 immunity-related genes confirmed that hypoxia dampens the up-regulation of flg22
354 response genes (Fig. 4B), including PRR-coding genes such as *FLS2* and *EFR*, through
355 mechanisms that appear to be mostly independent from the ERF-VIIs. Immunoblot analysis
356 of FLS2 protein levels using seedlings of a $FLS2_{pro}$*:FLS2-3xmyc-GFP* line (Robatzek et al.,
357 2006) further suggested that FLS2 protein levels are unchanged after 1 hr of combined
358 hypoxia/flg22 treatment compared to individual treatments (Fig. S5A). Phosphorylation of
359 MPK3 and MPK6 is reduced under combined hypoxia/flg22 treatment compared to flg22
360 treatment alone, with similar effects observed in the *erfVII* mutant (Fig. 4C, D and Fig. S5B).
361 In contrast, *MPK3/4/6* expression was not repressed under hypoxia/flg22 compared to flg22
362 treatment alone (Fig. S5C). Finally, callose deposition was significantly decreased under
363 combined hypoxia/flg22 conditions in Col-0 and *erfVII* seedlings, compared to treatment
364 with flg22 alone (NF) (Fig. 4E and Fig. S5D), with no statistically significant differences
365 between Col-0 and *erfVII.* Altogether, our data indicate that several aspects of PTI are
366 repressed under simultaneous hypoxia/flg22 treatments compared to flg22 alone, and that
367 these effects are mostly ERF-VII independent.
368

369 **Discussion**

370 In animals, the complex crosstalk between hypoxia and immunity has been known for
371 decades and some of the underlying mechanisms have been dissected in different cell types.
372 For example, using murine macrophages as a model system, hypoxia has been shown to

373 dampen innate immune signalling pathways (Rahat et al., 2011; Taylor and Colgan, 2017;
374 Weigert et al., 2018). In plants, it has been shown that infection with the necrotrophic
375 fungus *Botrytis cinerea* can result in localized hypoxic niches as a consequence of increased
376 respiration and/or water soaking (Valeri et al., 2021). Other pathogens trigger local hypoxic
377 environments *via* the formation of galls/tumors (e.g. *Agrobacterium tumefaciens*) (Kerpen
378 et al., 2019). In this context, the ERF-VII transcription factors have been shown to play a role
379 in the ability of plants to defend themselves (Gravot et al., 2016; Kerpen et al., 2019).
380 Despite these potential links between hypoxia and infection by necrotrophic and gall-
381 forming pathogens, the connection between hypoxia and innate immune signalling
382 pathways has not been investigated in detail. Here, we used transcriptomics datasets to
383 identify connections between hypoxia and PTI, and show that hypoxia represses PTI and
384 examined whether ERF-VIIs play a role in the crosstalk between hypoxia response and PTI.
385 The genome-wide comparison of the transcriptional changes induced by flg22
386 treatment in wild-type Col-0 and *a1a2* seedlings revealed that the flg22 transcriptional
387 response program includes sets of hypoxia response genes, and that this overlap is a
388 conserved feature, at least within the Brassicaceae (see model in Fig. 4F). Our
389 transcriptomic data with the *a1a2* mutant, that constitutively accumulates ERF-VII
390 transcription factors (Gibbs et al., 2011) suggested that ERF-VIIs could play a role in the
391 transcriptional regulation of some flg22-responsive genes. Despite the fact that a proportion
392 of these flg22-responsive genes were bound by HRE2 (Lee and Bailey-Serres, 2019), our RT-
393 qPCR data instead suggests that ERF-VIIs are unlikely to play a role.
394 A key question is whether the hypoxia-related genes identified in flg22
395 transcriptomics datasets are regulated due to the formation of a hypoxic environment
396 during PTI, or require alternative hypoxia-independent mechanisms for their regulation. Our
397 data indirectly suggest that flg22 treatment does not trigger hypoxia in seedlings, as we did
398 not detect the up-regulation of many well-characterized hypoxia marker genes, such as
399 *ALCOHOL DEHYDROGENASE1* (*ADH1*) or *PLANT CYSTEINE OXIDASE1* (*PCO1*). This is in
400 agreement with previous data suggesting that flg22 concentrations of up to 10 µM (a
401 concentration higher than those used in this study) are not sufficient to trigger local hypoxic
402 niches in 3-4-week old plants (Valeri et al., 2021). Hence, the regulation of common genes
403 by either hypoxia or flg22 treatment may not require the formation of a hypoxic
404 environment, but instead might involve other mechanisms.

405 Considering the overlap between the transcriptional responses to flg22 and hypoxia,
406 and also the fact that hypoxic niches form during infection by necrotrophic and gall-forming
407 pathogens (Kerpen et al., 2019; Valeri et al., 2021), we examined more carefully the
408 potential crosstalk between hypoxia and PTI by first comparing the genome-wide
409 transcriptional changes in wild-type seedlings treated with individual stresses (hypoxia or
410 flg22 alone) or combined hypoxia/flg22. The use of metrics developed to compare the
411 crosstalk between stresses (Tan et al., 2023) revealed that hypoxia represses the
412 transcriptional flg22-response program, and that this repression is particularly relevant for
413 genes that are down-regulated by flg22. Indeed, the negative suppression score was lower
414 for down-regulated genes (-0.16 compared to -0.031 for up-regulated genes), and
415 importantly was also within the same range as the suppression scores obtained when
416 combined abiotic stresses were applied to *Marchantia* (Tan et al., 2023). Unique features
417 associated with the response of wild-type seedlings to combined hypoxia/flg22 emerged in
418 our datasets, with over 900 unique DEGs upon hypoxia/flg22 treatment, compared to
419 hypoxia or flg22 treatments alone. The novel interaction score obtained for down-regulated
420 genes upon combined hypoxia/flg22 was higher than the novel interaction scores found for
421 the range of 18 combined abiotic stresses in *Marchantia* (Tan et al., 2023), thus suggesting
422 that the repression of specific sets of genes is an important and unique feature of plant
423 responses to combined hypoxia/flg22. These unique features include the repression of
424 developmental processes, which could correlate with a resource/allocation problem and
425 potential energy crisis that is typical of hypoxia stress. In addition, we observed the
426 repression of genes coding for enzymes (cytochromes P450) that use oxygen as co-
427 substrate, suggesting a limitation of enzymatic processes that consume oxygen (Fig. 4F).
428 Another unique feature of the combined hypoxia/flg22 response was the over-
429 representation of genes associated with transcription factors, with some families being up-
430 regulated (NAC, WRKY, bZIP), while others tended to be predominantly down-regulated
431 (bHLH, Zn finger, homeobox). Altogether, the data suggest that the coordination of plant
432 responses to combined hypoxia/flg22 requires the orchestration of gene expression changes
433 under the control of specific transcription factor families. Notably, some of the up-regulated
434 transcription factor families, such as NAC or WRKY, are typically associated with stress
435 responses (Shao et al., 2015). Interestingly, the WRKY22 transcription factor had previously
436 been identified as being up-regulated during submergence in the dark (which results in

437 hypoxia) and to play a role in the induction of plant defenses to pathogens following a 12-hr
438 dark submergence treatment (Hsu et al., 2013). These stress conditions are different from
439 our combined hypoxia/flg22 treatments. Nevertheless, we found WRKY22 up-regulated in
440 our hypoxia/flg22 dataset, together with 11 (out of 45) genes whose genomic regions were
441 shown to be bound by WRKY22 (Hsu et al., 2013). This indicates that WRKY22 may be a
442 regulator of plant responses to combined hypoxia/flg22.
443 Some of the transcription factor families that are mostly repressed (*e.g.* homeobox
444 transcription factors) are generally associated with developmental processes (Jeong et al.,
445 2012). This suggests again an increased need to regulate resource allocation under
446 combined stress, with a stronger prioritization of stress response pathways as opposed to
447 developmental processes. Our core findings with combined hypoxia/flg22 (*i.e.* the
448 preponderance of a novel transcriptional response, the relevance of transcription factors
449 and the stronger prioritization of stress responses) are reminiscent of previous findings in
450 studies with combined abiotic/biotic stresses (Atkinson and Urwin, 2012; Prasch and
451 Sonnewald, 2013; Rasmussen et al., 2013; Suzuki et al., 2014; Pandey et al., 2015; Zhang and
452 Sonnewald, 2017; Saijo and Loo, 2020). However, such studies have thus far focused on
453 combinations between pathogens and abiotic stresses such as heat and drought, and have
454 not included hypoxia.
455 Notably, the repression of PTI by hypoxia is not observed just at the transcriptional
456 level. Our data show that MAPK signalling and callose deposition are repressed under
457 combined hypoxia/flg22. In the case of MAPK, the inhibitory effects appear to be
458 independent of the transcriptional regulation of *MPK3/4/6*, and occurs either post-
459 transcriptionally on MPK proteins, or further upstream in the flg22-dependent signalling
460 events originating from FLS2. Similarly, the expression of genes encoding key PTI
461 components, such as the PRRs *FLS2* and *EFR*, is repressed under combined hypoxia/flg22
462 compared to flg22 alone. However, RT-qPCR analysis using *erfVII* mutants suggested that
463 these master regulators of the hypoxia response program do not play a major role in
464 regulating plant responses to combined hypoxia/flg22. Potential other candidates include
465 WRKY22 (Hsu et al., 2013) as discussed above, or the ZPR2 and VRN2 transcriptional
466 regulators, which are also known to be degraded by the N-degron pathway in an oxygen-
467 dependent manner (Gibbs et al., 2018; Weits et al., 2019; Labandera et al., 2020). VRN2
468 degradation also depends on the presence of nitric oxide (Gibbs et al., 2018), an important

469 signalling molecule induced in response to both hypoxia and PAMPs/pathogens (Mugnai et
470 al., 2012; Bleau and Spoel, 2021; Borrowman et al., 2023). The role of nitric oxide in
471 integrating hypoxia and immume signaling thus appears as an interesting focus for further
472 studies.

473 Connections and crosstalk between hypoxia response and immunity/plant defenses
474 are also likely to evolve in the course of development, as the levels of ERF-VIIs and the
475 regulation of innate immunity change with developmental stages and age (Kus et al., 2002;
476 Lozano-Duran and Zipfel, 2015; Giuntoli et al., 2017; Giuntoli and Perata, 2018; Zou et al.,
477 2018). Such developmentally-dependent crosstalk between abiotic and biotic stresses was
478 identified in the context of combined mild salt stress and pathogen infection with the
479 biotrophic oomycete *Hyaloperonospora arabidopsidis* or with the hemibiotrophic bacterium
480 *Pseudomonas syringae* (Berens et al., 2019). In the latter study, the hormonal crosstalk
481 between abscisic acid (ABA) and salicylic acid (SA) played an important age-dependent role.
482 The hypoxia/immunity crosstalk may also be particularly complex because, in contrast to
483 other abiotic stresses, hypoxia itself has a dual nature, in that it may be considered as either
484 a stress (*e.g.* during flooding; termed 'acute hypoxia' in this context), or a physiological
485 condition (*e.g.* in meristems, which are hypoxic; termed 'chronic hypoxia') (Loreti and
486 Perata, 2020; Weits et al., 2021). Hence, the output of the crosstalk between hypoxia and
487 immunity could differ between tissues and cell types, as observed in mammals (reviewed in
488 (Taylor and Colgan, 2017)) and as suggested by a recent single-cell RNA-seq study (Liu et al.,
489 2023).

490 Finally, combined hypoxia/flg22 treatment indicates that plants or tissues
491 experiencing acute hypoxia are likely to be more susceptible to pathogens. The latter is
492 important to explore and consider in terms of agricultural applications, as it suggests that
493 flooding may have a negative impact on the ability of plants to fight-off pathogens. This
494 could be exacerbated by the fact that flooding also causes an increased risk of pathogen
495 infection, likely as a result of increased dampness and changes to the soil and plants'
496 microbiome (Hartman and Tringe, 2019; Gschwend et al., 2020). Hence, the crosstalk
497 between hypoxia and immunity is a new trait to consider in our endeavour to generate
498 more climate resilient crops.
499

500 ## Materials and Methods

501 **Arabidopsis lines used**

502 *Arabidopsis thaliana* accession Columbia-0 (Col-0) was used for this study. Mutant lines
503 used are listed and described in Supplemental Table S1. *Arabidopsis* accession Wassilewskija
504 (Ws) was used as a flg22-insensitive control (Zipfel et al., 2004).

505

506 **Plant growth conditions**

507 *A. thaliana* plants were grown in 4-cell pots on a soil mixture containing a 5:3:2 ratio of
508 compost:vermiculite:perlite. The soil mixture was sterilized by autoclaving prior to use.
509 When axenic conditions were required, seedlings were grown in Petri dishes containing
510 0.5xMS medium (pH 5.7) and 6 g/L agar with 0.5% sucrose (w/v). Prior to sowing on agar
511 medium, seeds were surface-sterilized using the vapor-phase sterilization method (Lindsey
512 et al., 2017). Trays or plates were kept at 4°C for 3 days prior to transfer to growth rooms.

513

514 ***Arabidopsis thaliana* flg22 RNA-Seq experiments**

515 Seedlings were grown on 0.5xMS agar with 0.5% sucrose plates in continuous light at 20°C.
516 After 9 days of growth, 50 seedlings *per* genotype *per* treatment were transferred to 2 wells
517 of a 6-well plate, each containing 6 mL of 0.5xMS with 0.5% sucrose liquid medium and
518 returned to continuous light with gentle agitation at 120 rpm. 24 hrs after transfer, 1 µM
519 flg22 or an equivalent volume of water (mock treatment) were added to each well. After 1
520 hr, all seedlings were harvested in liquid nitrogen and stored at -80°C. After grinding, frozen
521 tissue was divided equally for RNA extraction (for RNA-seq) and for protein isolation
522 (proteomic analysis).

523

524 **RNA-seq for combined hypoxia/flg22 experiments**

525 Seedlings were grown on 0.5xMS agar supplemented with 0.5% sucrose in continuous light
526 at 20°C for 9 days. On day 9, five seedlings *per* genotype *per* treatment were transferred to
527 35 mm x 10 mm dishes, each containing 4 mL of 0.5xMS liquid medium and placed on a
528 shaker at 120 rpm overnight in continuous light conditions (20°C). On day 10, seedlings were
529 treated simultaneously with 100 nM flg22 or equivalent volume of water (mock), and with

530 hypoxia (in anaerojars) or normoxia at ambient O_2 levels. After 1 hr, the seedlings were
531 harvested in liquid nitrogen and stored at -80°C.
532
533 **Protein extraction and proteomics sample preparation**
534 Protein extraction buffer (2% SDS, 100 mM HEPES pH 7.5, 5 mM EDTA, Thermo Halt Cocktail
535 1:100) was added to the ground tissue, which originated from the same samples used for
536 RNA-seq (i.e. the powder was split in 2 for both RNA-seq and proteomics). The volume of
537 buffer added was 1 µL for 0.3 mg of tissue, with a minimum volume of 300 µL *per* sample.
538 Proteins were then denatured by heating samples at 70°C for 12 minutes and samples were
539 centrifuged at 2,500 x g for 10 minutes. The protein lysate was transferred to a fresh tube
540 and protein was quantified using the amido black protein quantification method (Schaffner
541 and Weissmann, 1973; Popov et al., 1975).
542 For proteome analysis, 20 µg each sample were treated with 0.5 µl benzonase (~26
543 U/µl) at 37°C for 30 min, reduced with 10 mM dithiothreitol (DTT) shaking at 37°C for 30 min
544 and alkylated with 50 mM chloroacetamide (CAA) at room temperature in the dark for
545 30 min. The reaction was quenched with an additional 50 mM DTT for 20 min before protein
546 purification with SP3-beads (Cytiva) as described previously (Hughes et al., 2019). The
547 samples were resuspended in 100 mM HEPES, 2.5 mM $CaCl_2$, pH 7.5 and digested with
548 trypsin (proteome:enzyme ratio 100:1 w/w) overnight at 37°C. Digested peptides were
549 desalted with self-packed C18 STAGE-tips (Rappsilber et al., 2007) and resuspended in 0.1%
550 formic acid (FA).
551
552 **Mass spectrometry and proteomics data analysis**
553 LC–MS/MS analysis was performed with an UltiMate 3000 RSCL nano-HPLC system
554 (Thermo) coupled to an Impact II Q-TOF mass spectrometer (Bruker) with a CaptiveSpray ion
555 source (Bruker) operated with an acetonitrile (ACN)-saturated nitrogen gas stream. For each
556 run, an estimated 1 µg peptides were loaded on an µPAC pillar array trap column (1 cm
557 length, PharmaFluidics) and separated on a µPAC pillar array analytical column (50 cm
558 flowpath, PharmaFluidics). Peptides were eluted using a 2 hr elution protocol that included
559 an 80 min separation gradient from 5% to 32.5% solvent B (solvent A: 0.1% FA, solvent B:
560 0.1% FA in ACN) at a flow rate of 600 nl min^{-1}, with columns temperated at 40°C. Tandem
561 mass spectra were acquired at 15 Hz in Data Independent Acquisition (DIA) mode, with 400–

562 1200 precursor m/z windows for MS1 and 32 windows of 25 m/z with 0.5 m/z overlap in a
563 range from 200–1750 m/z for MS2.
564 Peptide sequences were identified with DIA-NN (Demichev et al., 2020), version 1.8,
565 using a spectral library predicted from the UniProt *Arabidopsis thaliana* reference proteome
566 (UP000006548_3702, release 2021_02). Search settings were set to double-pass mode with
567 a precursor FDR of 1%, considering Cys carbamidomethylation as a fixed modification.
568 Downstream data analysis was performed using the Perseus software (Tyanova et al., 2016),
569 v.1.6.15.0. Data was log2-transformed and grouped by treatments and genotype in 4 groups
570 (*ate1 ate2* or wild type treated with flg22 or control). Multi-sample ANOVA (permutation-
571 based FDR<0.05) followed by Tukey's *post-hoc* test with FDR<0.05) as implemented in
572 Perseus was used to determine significant difference in abundance between the conditions.
573
574 **Flg22 seedling growth and root growth inhibition assays**
575 Seedlings were grown on 0.5xMS agar plates supplemented with 0.5% sucrose in continuous
576 light at 20°C.
577 For seedling growth inhibition assays: individual 5.5-day old seedlings were transferred to
578 one well of a 48-well plate containing 1 mL of liquid 0.5xMS medium supplemented with
579 100 nM flg22 (or equivalent volume of water (mock). For each condition and genotype, 8
580 seedlings were used in a given biological replicates. Seedlings were then grown with mild
581 shaking (120 rpm) in continuous light (20°C) for 7 days. To weigh the seedlings, all 8
582 seedlings for a given genotype and condition were harvested together on a paper towel to
583 remove any liquid and weighed together.
584 For root growth inhibition assays to compare Col-0 and *ate1 ate2*: 5.5-day old seedlings
585 were transferred to 0.5xMS with 1% agar plates that contained either a mock solution
586 (water) or 500 nM flg22 and grown vertically for 3 days in continuous light (20°C). Root
587 elongation during this 3-day period was measured using Image J.
588 For root growth inhibition assays under combined hypoxia/flg22: 5.5-day old seedlings were
589 transferred to 0.5xMS with 1% agar plates that contained either a mock solution (water) or
590 500 nM flg22, followed by vertical growth in short-day conditions (8 hrs light; 16 hrs dark)
591 for 48 hrs under normal oxygen conditions. Hypoxia treated seedlings were kept at 0.5%
592 oxygen (applied using PhO_2X Box (Baker Ruskinn)); plates kept vertical) for 48 hrs in short-
593 day conditions. Normoxia-treated seedlings were kept under normoxic and short-day

594 conditions for 48 hrs. After this 48-hr hypoxia/normoxia treatment, all seedlings were kept
595 vertical for an additional 3 days in short-day conditions and normoxia (*i.e.* recovery period).
596 Root elongation during the 3-day recovery period was determined using ImageJ.
597
598 **Reverse transcription quantitative PCR (RT-qPCR)**
599 RNA was reverse transcribed using RevertAid Reverse Transcriptase (Thermo Fisher) in the
600 presence of RiboLock RNase inhibitor (Thermo Fisher), oligo(dT)18 and 1 mM dNTP mixture
601 at 42°C for 45 minutes. qPCR reactions were carried out in a LightCycler 480 instrument
602 (Roche) using 1 µL of cDNA mixed with 1 µL of a primer pair mixture (1 µM final
603 concentration each), 5 µL 2X SYBR green master mix (Roche) and nuclease-free water added
604 to a final volume of 10 µL *per* well. The second derivative maximum method was used to
605 determine crossing point (Cp) values. Gene expression was calculated relative to a reference
606 gene with the comparative Ct method ($Cp_{reference\ gene} - Cp_{gene\ of\ interest}$ = deltaCp). Assuming a
607 PCR efficiency value of 2, relative expression was calculated as $2^{deltaCp}$. *MON1* (AT2G28390)
608 was used as a reference gene for RT-qPCRs (de Marchi et al., 2016). Primers used for RT-
609 qPCR analysis are listed in Supplemental Table S2.
610
611 **RNA-Sequencing, data processing and functional analysis**
612 Each RNA-seq experiment was conducted using samples from three biological replicates.
613 Total RNA was isolated using the Spectrum Total RNA kit (Merck), and RNA integrity was
614 assessed using an Agilent 2100 Bioanalyzer (Agilent). All RNA samples had RNA integrity
615 (RIN) values >7.0. Library preparation and paired-ended 100 bp next-generation sequencing
616 was performed by BGI (Hong Kong) using the BGI-seq PE100 platform. Data processing was
617 carried out by BGI using the filtering software SOAPnuke (including removal of reads
618 containing the adaptor; removal of reads whose N content is greater than 5%; and removal
619 of low-quality reads). The Hierarchical Indexing for Spliced Alignment of Transcripts (HISAT)
620 software was then used for mapping clean reads to the reference genome. Differential gene
621 expression was determined using DESeq2. Cut-offs of adj. *p*-value<0.05 and
622 |log2(FC)|>0.585 were applied to determine differentially expressed genes (DEGs).
623 Significant enrichment analysis of GO function on DEGs was carried out using the BiNGO
624 plug-in in Cytoscape. Overlap between datasets was determined using InteractiVenn

625 (Heberle et al., 2015), and statistical significance of the overlap between datasets was
626 calculated using 2x2 contingency tables and Chi-square tests.
627
628 **Callose deposition assays**
629 Seedlings were grown on 0.5xMS agar with 0.5% sucrose plates for 9 days under short-day
630 light conditions (8 hrs light; 16 hrs dark) at 20°C. After 9 days of growth, 5 seedlings *per*
631 genotype *per* treatment were transferred to 3 mL 0.5xMS liquid medium in 35 mm x 10 mm
632 petri dishes. These were placed on a shaker at 120 rpm in short-day conditions before the
633 dark period. On day 10, seedlings were treated for 24 hrs as follows: NM = normoxia
634 (ambient O_2) and mock treatment (addition of a volume of PBS equivalent to that of the
635 flg22 solution); NF = normoxia (ambient O_2) and flg22 (1 µM; prepared in PBS); HM =
636 hypoxia (5% O_2) and mock treatement; HF = hypoxia (5% O_2; applied using PhO_2X Box (Baker
637 Ruskinn)) and 1 µM flg22. After 24 hrs, treatment solutions were aspirated, 100% ethanol
638 was added and samples were returned to short days on a shaker at 120 rpm. After 24 hrs,
639 the ethanol was removed and seedlings were washed with 0.07 M PBS (pH 9). Seedlings
640 were stained using 0.01% (w/v) aniline blue in 0.07 M PBS (pH 9) for 2 hrs with constant
641 agitation at 120 rpm. Cotyledons were mounted on slides using 50% (v/v) glycerol and
642 imaged using fluorescent microscope under DAPI filter. Quantitation of callose deposits was
643 done as detailed in (Mason et al., 2020). Briefly, the Trainable Weka Segmentation (TWS)
644 plugin on Fiji was used to identify callose deposits while excluding background fluorescence
645 (*e.g.* vasculature or edges of tissue), by manually training the plugin using a set of callose
646 deposition pictures. Once trained, all pictures obtained were analyzed using the plugin and
647 the results depicting the identified puncta were quantified using the *Analyze Particles* tool in
648 Fiji.
649
650 **Immunoblots FLS2 and MPK**
651 Seedlings grown on 0.5xMS agar with 0.5% sucrose for 9 days in continuous light (20°C)
652 were transferred to 0.5xMS medium in 35 mm x 10 mm dishes so that there were 10-15
653 seedlings *per* genotype *per* treatment in each dish. These dishes were returned to
654 continuous light on a shaker at 120 rpm overnight. On day 10, seedlings were treated +/-
655 100 nM flg22 (mock = PBS) +/- hypoxia in anaerojars (normoxia = ambient O_2 levels) for 30
656 min or 1 hr for MAPK-phosphorylation and FLS2-GFP immunoblots, respectively. Seedlings

657 were collected on liquid nitrogen and protein was extracted by grinding tissue in liquid
658 nitrogen and adding 2xSDS loading buffer (Laemmli buffer) to the ground tissue in a 1:1
659 volume (μL):weight (mg) ratio. Proteins were denatured by heating samples to 95°C for 5
660 min followed by centrifuging at maximum speed for 10 min. The protein lysate was
661 collected and protein concentration was using the amido black method (Schaffner and
662 Weissmann, 1973; Popov et al., 1975). 30 μg of protein was loaded per well on 12% SDS-
663 PAGE gels for MAPK-phosphorylation immunoblots; 100 μg of protein was loaded per well
664 on 10% SDS-PAGE gels for FLS2-GFP immunoblots. Separated proteins were transferred
665 from gels to PVDF membrane. Equal protein loading was assessed through Ponceau S
666 staining (0.4% (w/v) Ponceau S, 10% (v/v) acetic acid in water)of the PVDF membrane.
667 Membrane was blocked with 5% milk in TBS-T or PBS-T (containing 0.05% (v/v) Tween-20)
668 for MAPK-phosphorylation and FLS2-GFP immunoblots, respectively. Blots were incubated
669 overnight at 4°C with appropriate primary antibody with constant rotation: anti-MAPK-
670 phosphorylation (Cell Signalling #4370S; 1:2,000); anti-GFP (Merck #1181446001; 1:1,000).
671 Blots were washed with TBS-T or PBS-T for 3 x 5 minutes for MAPK-phosphorylation and
672 FLS2-GFP blots, respectively, before and after incubation of blots with appropriate
673 secondary antibody (anti-rabbit HRP (Merck #A0545; 1:50,000); anti-mouse HRP (Merck
674 #A9044; 1:10,000)) for 2 hrs at room temperature . WesternBright ECL substrate (Advansta)
675 was used and immunoblots were imaged using the G:BOX gel documentation system and
676 the GeneSys software.
677
678
679 **Detection of reactive oxygen species**
680 Flg22-induced reactive oxygen species (ROS) were detected using a luminol-based approach.
681 Seeds were sown on 0.5xMS agar plates containing 0.5% sucrose, and stratified at 4°C for 3
682 days. Plates were transferred to a growth chamber at 20°C with 9 hrs of light *per* day. After
683 7 days of growth, individual seedlings were carefully moved to expanded Jiffy-7 (44 mm)
684 pellets and grown in the same conditions for a further 3 weeks. Discs were taken from
685 leaves of 4-week-old plants with a cork borer (1 cm diameter). Leaf discs were then carefully
686 divided in 4 equal-sized quarters with a razor blade. Each quarter-disc was placed into a
687 separate well of a white Sterilin 96-well plate (ThermoScientific) containing 200 μL dH_2O
688 with the abaxial leaf surface facing upwards. The plate was then returned to the growth

689 room for a recovery period of at least 3 hours. 100x stock solutions of luminol (Merck) (17.7
690 mg/mL in 200 mM KOH) and horseradish peroxidase (HRP) (Fisher Scientific) (10 mg/mL in
691 dH_2O) were prepared fresh. 60 µL of a luminescence solution containing 2.8 µL 100X
692 luminol, 2.8 µL 100X HRP and 54.4 µL dH_2O was added to each well using a multichannel
693 pipette. The plate was then transferred to a POLARstar Omega microplate reader (BMG
694 LABTECH) and luminescence was detected for 15 minutes to establish a baseline
695 measurement. After this time, 20 µL of flg22 solution (initial concentration: 1.4 µM; final
696 concentration: 100 mM) was added to each well. Luminescence was detected every 2
697 minutes after addition of flg22.

Figures and Figure legends

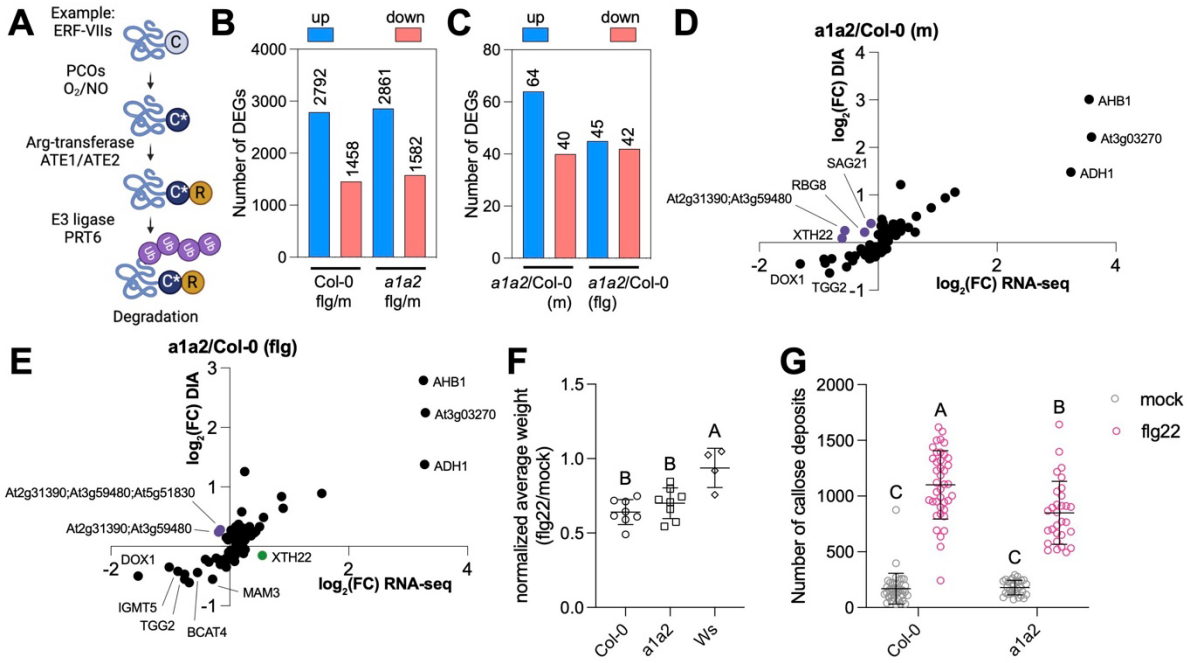

Figure 1: Response of *a1a2* mutant and wild-type Col-0 seedlings to flg22. (A) The oxygen-dependent Arg/N-degron pathway. O_2: oxygen; NO: nitric oxide. **(B)** Number of up and down-regulated DEGs when comparing flg22 to mock-treated samples (flg/m) for wild-type (Col-0) and *a1a2* (a1a2) mutant seedlings. **(C)** Number of up and down-regulated DEGs when comparing *a1a2* to wild-type Col-0 seedlings, either mock (a1a2/Col-0 (m)) or flg22-treated (a1a2/Col-0 (flg)). **(D)** Comparison of differential protein accumulation and differential gene expression in mock-treated Col-0 and *a1a2* seedlings. **(E)** Comparison of differential protein accumulation and differential expression in flg22-treated Col-0 and *a1a2* seedlings. (D) and (E) Purple: lower mRNA levels and higher protein accumulation in *a1a2* compared to the wild type. Green: higher expression in *a1a2* seedlings, but lower protein levels in this mutant compared to the wild type. The $\log_2$ of the fold changes (FC) are shown. **(F)** Seedling growth inhibition assays. Ws: Wassilewskija (flg22-insensitive control (Zipfel et al., 2004)). Means and standard deviations are shown from 8 independent replicates (8 seedlings/genotype/replicate). Results of statistical tests are shown using the compact letter display (CLD) format after one-way ANOVA with Tukey's multiple comparison. **(G)** Quantitation of callose deposits following flg22 treatment. Means and standard deviations from 4 and 3 biological replicates are shown for Col-0 and *a1a2*, respectively, with 10

717 seedlings/replicate/condition. The results of two-way ANOVA and Tukey's multiple

718 comparison tests are shown using CLD.

719

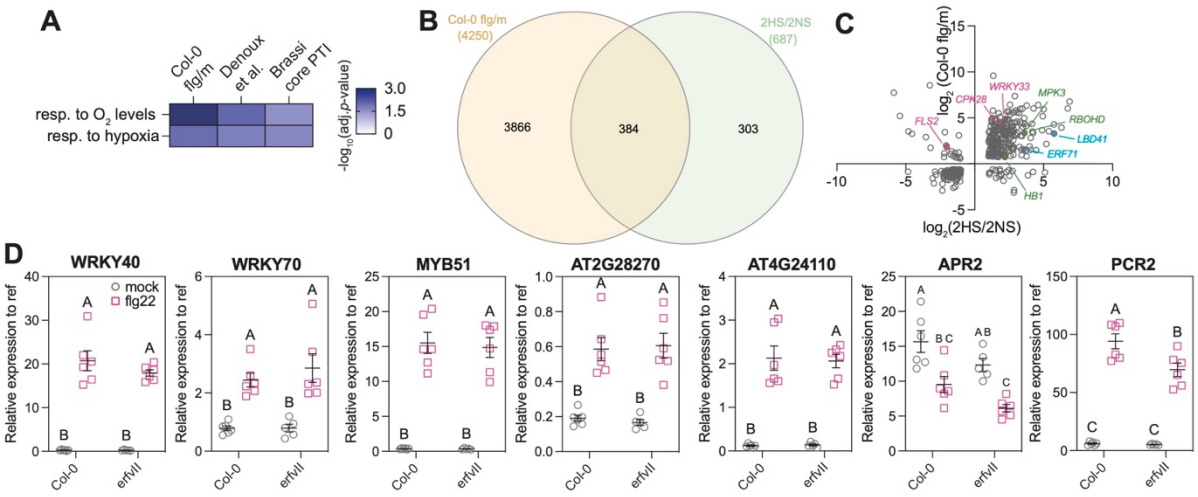

Figure 2: Overlap between the flg22 and hypoxia transcriptional response programs. (A) Enrichment for GO categories associated with oxygen levels in different datasets: Col-0 flg/m (this study); Denoux *et al.* (Denoux et al., 2008) and Brassicaceae core PTI (Winkelmuller et al., 2021). The -$\log_{10}$ of the corrected *p*-values are shown for the GO categories 'response to oxygen levels' (GO#70482) and 'response to hypoxia' (GO#1666). See also Supplemental Dataset 1. **(B)** Overlap between flg22 response genes identified in Col-0 and differentially regulated genes after 2 hrs of hypoxia (2HS/2NS; O_2<2%; cut-off applied: |log(FC)|>1.0 and FDR<0.05) (Lee and Bailey-Serres, 2019). **(C)** Comparison of the directionality and amplitude of gene expression change for the 384 genes common to Col-0 flg/m and 2HS/2NS. **(D)** Expression analysis using RT-qPCR of selected genes regulated by both hypoxia and flg22 treatments in wild-type Col-0 and *erfVII* quintuple mutant seedlings mock and flg22-treated. Mean and SEM from 6 biological replicates are shown. The results of two-way ANOVA and Tukey's multiple comparison tests are shown using CLD.

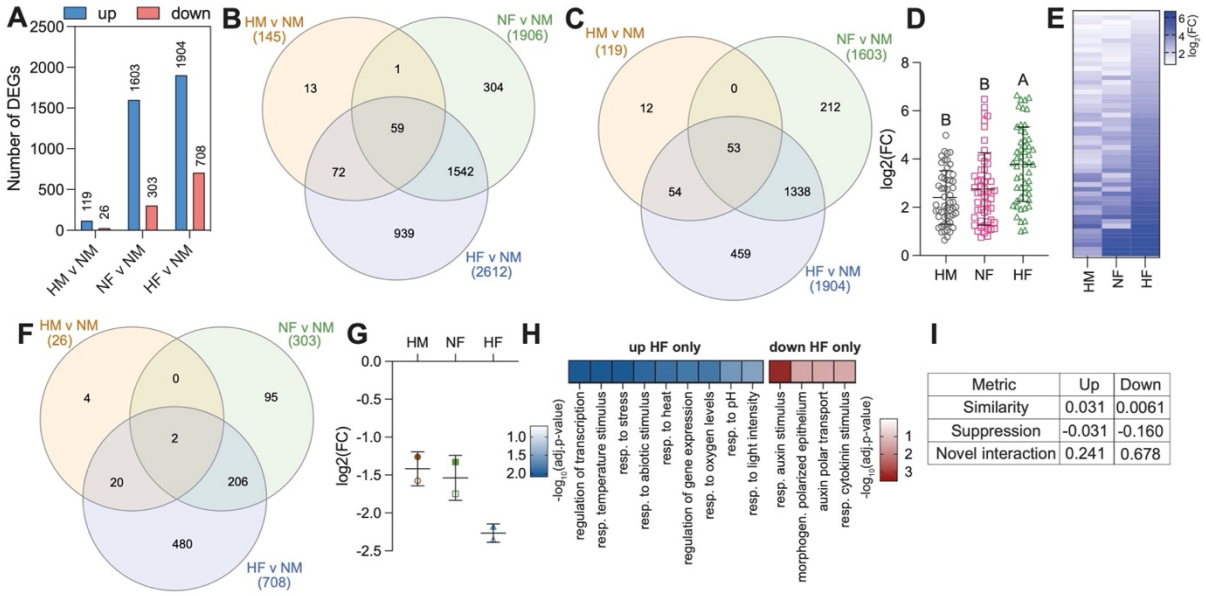

Metric	Up	Down
Similarity	0.031	0.0061
Suppression	-0.031	-0.160
Novel interaction	0.241	0.678

Figure 3: Effects of combined hypoxia/flg22 treatments on genome-wide transcription. (A) Number of up- and down-regulated genes. NM: normoxia/mock; HM: hypoxia/mock; NF: normoxia/flg22; HF: hypoxia/flg22. **(B)** Overlap between the 3 different datasets using all DEGs. **(C)** Overlap between the up-regulated DEGs in each of the 3 datasets. **(D)** Average expression of the 53 up-regulated DEGs common to all 3 datasets. Results of statistical tests are shown after one-way ANOVA with Tukey's multiple comparison. **(E)** Heatmap showing the $\log_2$(FC) in HM, NF and HF-treated seedlings for the 53 up-regulated DEGs common to all 3 datasets. **(F)** Overlap between the down-regulated DEGs. **(G)** Average expression of the 2 down-regulated DEGs common to all 3 datasets. Each gene is respectively represented with filled or open symbols. **(H)** Selected GO terms enriched (corrected *p*-value<0.05) amongst uniquely up- and down-regulated DEGs upon combined hypoxia/flg22. See Suppl. Dataset 5 for full list of GO terms. **(I)** Metrics to characterize the transcriptional interaction between individual (hypoxia or flg22) stresses and combined hypoxia/flg22 treatment (see Fig. S4 for calculations).

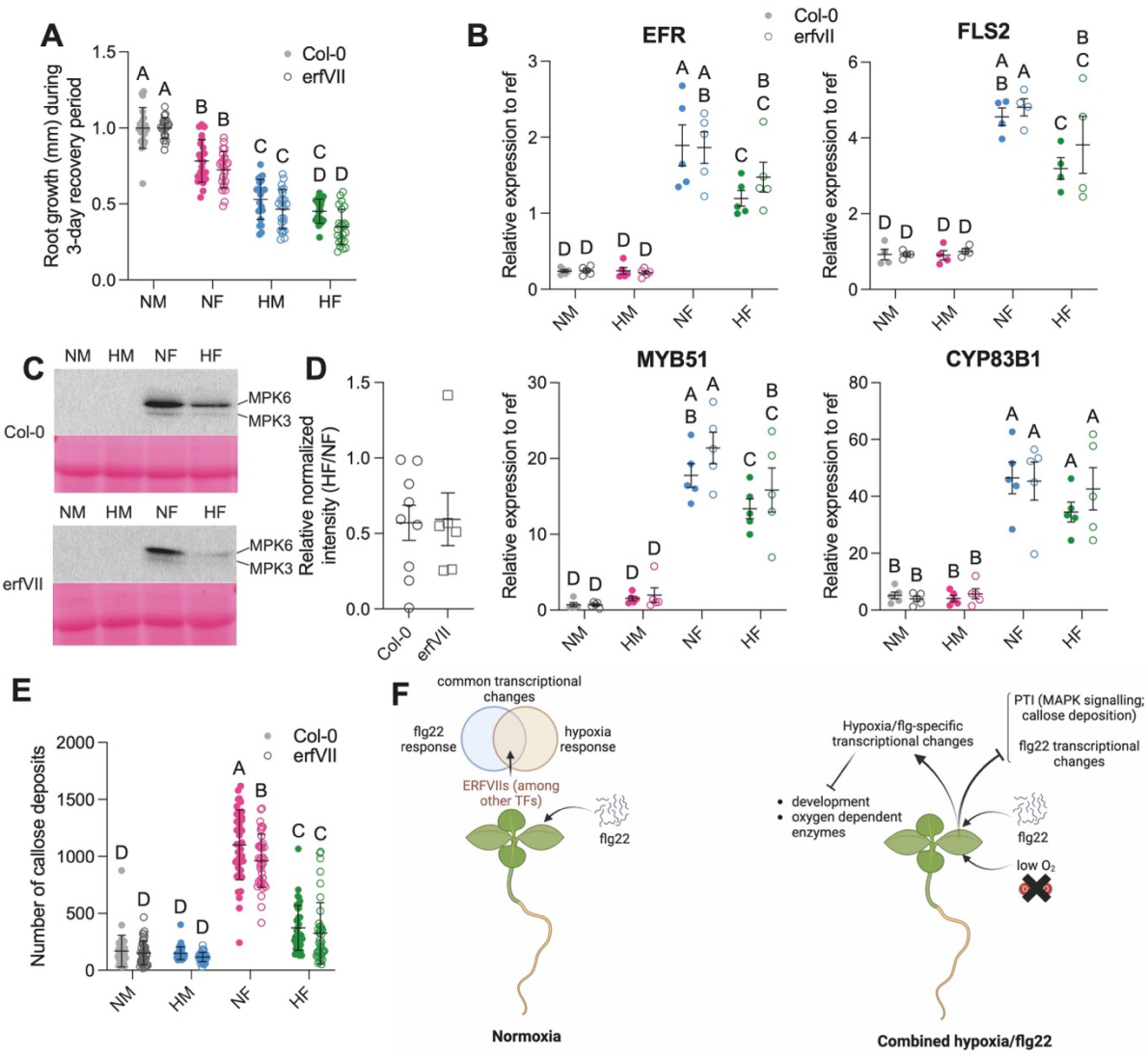

Figure 4: Repression of PTI by hypoxia in combined hypoxia/flg22 experiments. (A) Root growth inhibition assays with wild-type (Col-0) and *erfVII* mutant seedlings under combined hypoxia/flg22 treatment. Means and standard deviations of 4 biological replicates with 5-6 seedlings/genotype/condition in each biological replicate are shown. The results of statistical tests (two-way ANOVA with Tukey's test) are shown. Note that the Col-0 NM and Col-0 NF data is also shown in Fig. 1E. **(B)** Transcriptional suppression of immunity-related genes under combined hypoxia/flg22 treatment compared to normoxia/flg22 in Col-0 and *erfVII*. Means and SEM from 5 biological replicates are shown. The results of two-way ANOVA and Fisher's test are shown. **(C)** Anti-phosphorylated MPK immunoblots using Col-0 and *erfVII* mutant seedlings. See also Fig. S5. **(D)** Relative intensity of MPK signals under combined hypoxia/flg22 compared to normoxia/flg22 after normalization with Ponceau intensity. Mean and SEM of 9 (Col-0) and 6 (*erfVII*) biological replicates are shown. **(E)**

764 Quantitation from callose deposition experiments. Mean and standard deviation from 4
765 biological replicates are shown, with 10 seedlings/genotype/condition in each biological
766 replicate. The results of two-way ANOVA and Tukey's tests are shown. **(F)** Model
767 summarizing the crosstalk between hypoxia and PTI under normoxia, and upon combined
768 hypoxia/flg22.
769
770

Acknowledgements

We thank Prof. Silke Robatzek for sharing the *FLS2$_{pro}$:FLS2-3xmyc-GFP* line. This work was funded by grant 20/FFP-P/8433 from Science Foundation Ireland to EG. BCM was supported by an Irish Research Council PhD scholarship (GOIPG/2017/2); CMD was supported by an Irish Research Council PhD scholarship (GOIPG/2022/878) and by a PhD scholarship from the Kathleen Lonsdale Institute for Human Health Research (Maynooth University). Work in PFH lab was funded by the Deutsche Forschungsgemeinschaft (DFG, German Research Foundation, SFB1403 – Project-ID 414786233) and under Germany's Excellence Strategy (CIBSS – EXC-2189 – Project ID 390939984). The authors confirm that they have no conflict of interest.

Authors contributions

BCM, CMD, MM, PG, PFH and EG designed the work, conducted experiments, analyzed data and wrote the manuscript.

Data Sharing

All data from this study are included in the article and/or in the supporting information. All lines are also available upon request. RNA-seq data have been deposited with the Gene Expression Omnibus (GEO) repository (at http://www.ncbi.nlm.nih.gov/) under GSE246173 and GSE246848. *Note to reviewers*: the data has been submitted and the authors are waiting for publication before release. Reviewer access can be requested. *Note to reviewers*: the RNA-seq data has been submitted and the authors are waiting for publication before public release. Reviewer access can be requested). The mass spectrometry proteomics data have been deposited to the ProteomeXchange Consortium (Deutsch et al., 2023) via the PRIDE (Perez-Riverol et al., 2022) partner repository with the dataset identifier PXD046263 (Reviewer account username: reviewer_pxd046263@ebi.ac.uk; Password: JdeljrD3).

References

Abbas M, Berckhan S, Rooney DJ, Gibbs DJ, Vicente Conde J, Sousa Correia C, Bassel GW, Marin-de la Rosa N, Leon J, Alabadi D, Blazquez MA, Holdsworth MJ (2015) Oxygen sensing coordinates photomorphogenesis to facilitate seedling survival. Curr Biol **25:** 1483-1488

Albrecht G, Mustroph A (2003) Sucrose Utilization via Invertase and Sucrose Synthase with Respect to Accumulation of Cellulose and Callose Synthesis in Wheat Roots under Oxygen Deficiency. Russian Journal of Plant Physiology **50:** 813-820

Atkinson NJ, Urwin PE (2012) The interaction of plant biotic and abiotic stresses: from genes to the field. J Exp Bot **63:** 3523-3543

Berens ML, Wolinska KW, Spaepen S, Ziegler J, Nobori T, Nair A, Kruler V, Winkelmuller TM, Wang Y, Mine A, Becker D, Garrido-Oter R, Schulze-Lefert P, Tsuda K (2019) Balancing trade-offs between biotic and abiotic stress responses through leaf age-dependent variation in stress hormone cross-talk. Proc Natl Acad Sci U S A **116:** 2364-2373

Bleau JR, Spoel SH (2021) Selective redox signaling shapes plant-pathogen interactions. Plant Physiol **186:** 53-65

Borrowman S, Kapuganti JG, Loake GJ (2023) Expanding roles for S-nitrosylation in the regulation of plant immunity. Free Radic Biol Med **194:** 357-368

Clay NK, Adio AM, Denoux C, Jander G, Ausubel FM (2009) Glucosinolate metabolites required for an Arabidopsis innate immune response. Science **323:** 95-101

de Marchi R, Sorel M, Mooney B, Fudal I, Goslin K, Kwasniewska K, Ryan PT, Pfalz M, Kroymann J, Pollmann S, Feechan A, Wellmer F, Rivas S, Graciet E (2016) The N-end rule pathway regulates pathogen responses in plants. Sci Rep **6:** 26020

Demichev V, Messner CB, Vernardis SI, Lilley KS, Ralser M (2020) DIA-NN: neural networks and interference correction enable deep proteome coverage in high throughput. Nat Methods **17:** 41-44

Denoux C, Galletti R, Mammarella N, Gopalan S, Werck D, De Lorenzo G, Ferrari S, Ausubel FM, Dewdney J (2008) Activation of defense response pathways by OGs and Flg22 elicitors in Arabidopsis seedlings. Mol Plant **1:** 423-445

Deutsch EW, Bandeira N, Perez-Riverol Y, Sharma V, Carver JJ, Mendoza L, Kundu DJ, Wang S, Bandla C, Kamatchinathan S, Hewapathirana S, Pullman BS, Wertz J, Sun Z, Kawano S, Okuda S, Watanabe Y, MacLean B, MacCoss MJ, Zhu Y, Ishihama Y, Vizcaino JA (2023) The ProteomeXchange consortium at 10 years: 2023 update. Nucleic Acids Res **51:** D1539-D1548

Dissmeyer N (2019) Conditional Protein Function via N-Degron Pathway-Mediated Proteostasis in Stress Physiology. Annu Rev Plant Biol **70:** 83-117

Garzon M, Eifler K, Faust A, Scheel H, Hofmann K, Koncz C, Yephremov A, Bachmair A (2007) PRT6/At5g02310 encodes an Arabidopsis ubiquitin ligase of the N-end rule pathway with arginine specificity and is not the CER3 locus. FEBS Lett **581:** 3189-3196

Gibbs DJ, Lee SC, Isa NM, Gramuglia S, Fukao T, Bassel GW, Correia CS, Corbineau F, Theodoulou FL, Bailey-Serres J, Holdsworth MJ (2011) Homeostatic response to hypoxia is regulated by the N-end rule pathway in plants. Nature **479:** 415-418

Gibbs DJ, Md Isa N, Movahedi M, Lozano-Juste J, Mendiondo GM, Berckhan S, Marin-de la Rosa N, Vicente Conde J, Sousa Correia C, Pearce SP, Bassel GW, Hamali B, Talloji P,

845 **Tome DF, Coego A, Beynon J, Alabadi D, Bachmair A, Leon J, Gray JE, Theodoulou**
846 **FL, Holdsworth MJ** (2014) Nitric oxide sensing in plants is mediated by proteolytic
847 control of group VII ERF transcription factors. Mol Cell **53:** 369-379
848 **Gibbs DJ, Tedds HM, Labandera AM, Bailey M, White MD, Hartman S, Sprigg C, Mogg SL,**
849 **Osborne R, Dambire C, Boeckx T, Paling Z, Voesenek L, Flashman E, Holdsworth MJ**
850 (2018) Oxygen-dependent proteolysis regulates the stability of angiosperm
851 polycomb repressive complex 2 subunit VERNALIZATION 2. Nat Commun **9:** 5438
852 **Giuntoli B, Perata P** (2018) Group VII Ethylene Response Factors in Arabidopsis: Regulation
853 and Physiological Roles. Plant Physiol **176:** 1143-1155
854 **Giuntoli B, Shukla V, Maggiorelli F, Giorgi FM, Lombardi L, Perata P, Licausi F** (2017) Age-
855 dependent regulation of ERF-VII transcription factor activity in Arabidopsis thaliana.
856 Plant Cell Environ **40:** 2333-2346
857 **Graciet E, Walter F, Maoileidigh DO, Pollmann S, Meyerowitz EM, Varshavsky A, Wellmer**
858 **F** (2009) The N-end rule pathway controls multiple functions during Arabidopsis
859 shoot and leaf development. Proc Natl Acad Sci U S A **106:** 13618-13623
860 **Gravot A, Richard G, Lime T, Lemarie S, Jubault M, Lariagon C, Lemoine J, Vicente J,**
861 **Robert-Seilaniantz A, Holdsworth MJ, Manzanares-Dauleux MJ** (2016) Hypoxia
862 response in Arabidopsis roots infected by Plasmodiophora brassicae supports the
863 development of clubroot. BMC Plant Biol **16:** 251
864 **Gschwend F, Aregger K, Gramlich A, Walter T, Widmer F** (2020) Periodic waterlogging
865 consistently shapes agricultural soil microbiomes by promoting specific taxa. Applied
866 Soil Ecology **155:** 103623
867 **Hartman K, Tringe SG** (2019) Interactions between plants and soil shaping the root
868 microbiome under abiotic stress. Biochem J **476:** 2705-2724
869 **Heberle H, Meirelles GV, da Silva FR, Telles GP, Minghim R** (2015) InteractiVenn: a web-
870 based tool for the analysis of sets through Venn diagrams. BMC Bioinformatics **16:**
871 169
872 **Holdsworth MJ, Vicente J, Sharma G, Abbas M, Zubrycka A** (2020) The plant N-degron
873 pathways of ubiquitin-mediated proteolysis. J Integr Plant Biol **62:** 70-89
874 **Holman TJ, Jones PD, Russell L, Medhurst A, Ubeda Tomas S, Talloji P, Marquez J,**
875 **Schmuths H, Tung SA, Taylor I, Footitt S, Bachmair A, Theodoulou FL, Holdsworth**
876 **MJ** (2009) The N-end rule pathway promotes seed germination and establishment
877 through removal of ABA sensitivity in Arabidopsis. Proc Natl Acad Sci U S A **106:**
878 4549-4554
879 **Hsu FC, Chou MY, Chou SJ, Li YR, Peng HP, Shih MC** (2013) Submergence confers immunity
880 mediated by the WRKY22 transcription factor in Arabidopsis. Plant Cell **25:** 2699-
881 2713
882 **Hughes CS, Moggridge S, Muller T, Sorensen PH, Morin GB, Krijgsveld J** (2019) Single-pot,
883 solid-phase-enhanced sample preparation for proteomics experiments. Nat Protoc
884 **14:** 68-85
885 **Jeong S, Volny M, Lukowitz W** (2012) Axis formation in Arabidopsis - transcription factors
886 tell their side of the story. Curr Opin Plant Biol **15:** 4-9
887 **Kerpen L, Niccolini L, Licausi F, van Dongen JT, Weits DA** (2019) Hypoxic Conditions in
888 Crown Galls Induce Plant Anaerobic Responses That Support Tumor Proliferation.
889 Front Plant Sci **10:** 56

890 **Kus JV, Zaton K, Sarkar R, Cameron RK** (2002) Age-related resistance in Arabidopsis is a
891 developmentally regulated defense response to Pseudomonas syringae. Plant Cell
892 **14:** 479-490
893 **Labandera AM, Tedds HM, Bailey M, Sprigg C, Etherington RD, Akintewe O, Kalleechurn G,**
894 **Holdsworth MJ, Gibbs DJ** (2020) The PRT6 N-degron pathway restricts
895 VERNALIZATION 2 to endogenous hypoxic niches to modulate plant development.
896 New Phytol
897 **Lee TA, Bailey-Serres J** (2019) Integrative Analysis from the Epigenome to Translatome
898 Uncovers Patterns of Dominant Nuclear Regulation during Transient Stress. Plant Cell
899 **31:** 2573-2595
900 **Licausi F, Kosmacz M, Weits DA, Giuntoli B, Giorgi FM, Voesenek LA, Perata P, van Dongen**
901 **JT** (2011) Oxygen sensing in plants is mediated by an N-end rule pathway for protein
902 destabilization. Nature **479:** 419-422
903 **Lindsey BE, 3rd, Rivero L, Calhoun CS, Grotewold E, Brkljacic J** (2017) Standardized Method
904 for High-throughput Sterilization of Arabidopsis Seeds. J Vis Exp
905 **Liu Z, Zhou Y, Liu Y, Qin A, Sun S, Liu H, Yang J, Hu M, Xie Y, Song X, Gao P, Guo E, Wang S,**
906 **Herrera-Estrella L, Tran L-S, Sun X** (2023) Single-Cell RNA-Sequencing Reveals the
907 Generation of New Immune Response-Induced Cells with Novel Role in Arabidopsis
908 thaliana Response to the Bacterial Flagellin Epitope flg22. .
909 http://dx.doi.org/10.2139/ssrn.4548674
910 **Loreti E, Perata P** (2020) The Many Facets of Hypoxia in Plants. Plants (Basel) **9**
911 **Lozano-Duran R, Zipfel C** (2015) Trade-off between growth and immunity: role of
912 brassinosteroids. Trends Plant Sci **20:** 12-19
913 **Luna E, Pastor V, Robert J, Flors V, Mauch-Mani B, Ton J** (2011) Callose deposition: a
914 multifaceted plant defense response. Mol Plant Microbe Interact **24:** 183-193
915 **Mason KN, Ekanayake G, Heese A** (2020) Staining and automated image quantification of
916 callose in Arabidopsis cotyledons and leaves. Methods Cell Biol **160:** 181-199
917 **Miricescu A, Goslin K, Graciet E** (2018) Ubiquitylation in plants: signaling hub for the
918 integration of environmental signals. J Exp Bot **69:** 4511-4527
919 **Mugnai S, Azzarello E, Baluska F, Mancuso S** (2012) Local root apex hypoxia induces NO-
920 mediated hypoxic acclimation of the entire root. Plant Cell Physiol **53:** 912-920
921 **Mustroph A, Zanetti ME, Jang CJ, Holtan HE, Repetti PP, Galbraith DW, Girke T, Bailey-**
922 **Serres J** (2009) Profiling translatomes of discrete cell populations resolves altered
923 cellular priorities during hypoxia in Arabidopsis. Proc Natl Acad Sci U S A **106:** 18843-
924 18848
925 **Nagels Durand A, Pauwels L, Goossens A** (2016) The Ubiquitin System and Jasmonate
926 Signaling. Plants (Basel) **5**
927 **Pandey P, Ramegowda V, Senthil-Kumar M** (2015) Shared and unique responses of plants
928 to multiple individual stresses and stress combinations: physiological and molecular
929 mechanisms. Front Plant Sci **6:** 723
930 **Pauwels L, Ritter A, Goossens J, Durand AN, Liu H, Gu Y, Geerinck J, Boter M, Vanden**
931 **Bossche R, De Clercq R, Van Leene J, Gevaert K, De Jaeger G, Solano R, Stone S,**
932 **Innes RW, Callis J, Goossens A** (2015) The RING E3 Ligase KEEP ON GOING
933 Modulates JASMONATE ZIM-DOMAIN12 Stability. Plant Physiol **169:** 1405-1417
934 **Perez-Riverol Y, Bai J, Bandla C, Garcia-Seisdedos D, Hewapathirana S, Kamatchinathan S,**
935 **Kundu DJ, Prakash A, Frericks-Zipper A, Eisenacher M, Walzer M, Wang S, Brazma**

936 **A, Vizcaino JA** (2022) The PRIDE database resources in 2022: a hub for mass
937 spectrometry-based proteomics evidences. Nucleic Acids Res **50:** D543-D552
938 **Popov N, Schmitt M, Schulzeck S, Matthies H** (1975) [Reliable micromethod for
939 determination of the protein content in tissue homogenates]. Acta Biol Med Ger **34:**
940 1441-1446
941 **Prasch CM, Sonnewald U** (2013) Simultaneous application of heat, drought, and virus to
942 Arabidopsis plants reveals significant shifts in signaling networks. Plant Physiol **162:**
943 1849-1866
944 **Rahat MA, Bitterman H, Lahat N** (2011) Molecular mechanisms regulating macrophage
945 response to hypoxia. Front Immunol **2:** 45
946 **Rappsilber J, Mann M, Ishihama Y** (2007) Protocol for micro-purification, enrichment, pre-
947 fractionation and storage of peptides for proteomics using StageTips. Nat Protoc **2:**
948 1896-1906
949 **Rasmussen S, Barah P, Suarez-Rodriguez MC, Bressendorff S, Friis P, Costantino P, Bones**
950 **AM, Nielsen HB, Mundy J** (2013) Transcriptome responses to combinations of
951 stresses in Arabidopsis. Plant Physiol **161:** 1783-1794
952 **Reynoso MA, Kajala K, Bajic M, West DA, Pauluzzi G, Yao AI, Hatch K, Zumstein K,**
953 **Woodhouse M, Rodriguez-Medina J, Sinha N, Brady SM, Deal RB, Bailey-Serres J**
954 (2019) Evolutionary flexibility in flooding response circuitry in angiosperms. Science
955 **365:** 1291-1295
956 **Robatzek S, Chinchilla D, Boller T** (2006) Ligand-induced endocytosis of the pattern
957 recognition receptor FLS2 in Arabidopsis. Genes Dev **20:** 537-542
958 **Sadanandom A, Bailey M, Ewan R, Lee J, Nelis S** (2012) The ubiquitin-proteasome system:
959 central modifier of plant signalling. New Phytol **196:** 13-28
960 **Saijo Y, Loo EP** (2020) Plant immunity in signal integration between biotic and abiotic stress
961 responses. New Phytol **225:** 87-104
962 **Salleh FM, Evans K, Goodall B, Machin H, Mowla SB, Mur LA, Runions J, Theodoulou FL,**
963 **Foyer CH, Rogers HJ** (2012) A novel function for a redox-related LEA protein
964 (SAG21/AtLEA5) in root development and biotic stress responses. Plant Cell Environ
965 **35:** 418-429
966 **Schaffner W, Weissmann C** (1973) A rapid, sensitive, and specific method for the
967 determination of protein in dilute solution. Anal Biochem **56:** 502-514
968 **Shao H, Wang H, Tang X** (2015) NAC transcription factors in plant multiple abiotic stress
969 responses: progress and prospects. Front Plant Sci **6:** 902
970 **Stone SL** (2014) The role of ubiquitin and the 26S proteasome in plant abiotic stress
971 signaling. Front Plant Sci **5:** 135
972 **Subbaiah CC, Sachs MM** (2001) Altered patterns of sucrose synthase phosphorylation and
973 localization precede callose induction and root tip death in anoxic maize seedlings.
974 Plant Physiol **125:** 585-594
975 **Suzuki N, Rivero RM, Shulaev V, Blumwald E, Mittler R** (2014) Abiotic and biotic stress
976 combinations. New Phytol **203:** 32-43
977 **Tan QW, Lim PK, Chen Z, Pasha A, Provart N, Arend M, Nikoloski Z, Mutwil M** (2023) Cross-
978 stress gene expression atlas of Marchantia polymorpha reveals the hierarchy and
979 regulatory principles of abiotic stress responses. Nat Commun **14:** 986
980 **Taylor CT, Colgan SP** (2017) Regulation of immunity and inflammation by hypoxia in
981 immunological niches. Nat Rev Immunol **17:** 774-785

982 **Till CJ, Vicente J, Zhang H, Oszvald M, Deery MJ, Pastor V, Lilley KS, Ray RV, Theodoulou**
983 **FL, Holdsworth MJ** (2019) The Arabidopsis thaliana N-recognin E3 ligase
984 PROTEOLYSIS1 influences the immune response. Plant Direct **3:** e00194
985 **Tyanova S, Temu T, Sinitcyn P, Carlson A, Hein MY, Geiger T, Mann M, Cox J** (2016) The
986 Perseus computational platform for comprehensive analysis of (prote)omics data.
987 Nat Methods **13:** 731-740
988 **Valeri MC, Novi G, Weits DA, Mensuali A, Perata P, Loreti E** (2021) Botrytis cinerea induces
989 local hypoxia in Arabidopsis leaves. New Phytol **229:** 173-185
990 **Varshavsky A** (2019) N-degron and C-degron pathways of protein degradation. Proc Natl
991 Acad Sci U S A **116:** 358-366
992 **Vicente J, Mendiondo GM, Movahedi M, Peirats-Llobet M, Juan YT, Shen YY, Dambire C,**
993 **Smart K, Rodriguez PL, Charng YY, Gray JE, Holdsworth MJ** (2017) The Cys-Arg/N-
994 End Rule Pathway Is a General Sensor of Abiotic Stress in Flowering Plants. Curr Biol
995 **27:** 3183-3190 e3184
996 **Vicente J, Mendiondo GM, Pauwels J, Pastor V, Izquierdo Y, Naumann C, Movahedi M,**
997 **Rooney D, Gibbs DJ, Smart K, Bachmair A, Gray JE, Dissmeyer N, Castresana C, Ray**
998 **RV, Gevaert K, Holdsworth MJ** (2019) Distinct branches of the N-end rule pathway
999 modulate the plant immune response. New Phytol **221:** 988-1000
1000 **Wang Z, Orosa-Puente B, Nomoto M, Grey H, Potuschak T, Matsuura T, Mori IC, Tada Y,**
1001 **Genschik P, Spoel SH** (2022) Proteasome-associated ubiquitin ligase relays target
1002 plant hormone-specific transcriptional activators. Sci Adv **8:** eabn4466
1003 **Weigert A, von Knethen A, Fuhrmann D, Dehne N, Brune B** (2018) Redox-signals and
1004 macrophage biology. Mol Aspects Med **63:** 70-87
1005 **Weits DA, Giuntoli B, Kosmacz M, Parlanti S, Hubberten HM, Riegler H, Hoefgen R, Perata**
1006 **P, van Dongen JT, Licausi F** (2014) Plant cysteine oxidases control the oxygen-
1007 dependent branch of the N-end-rule pathway. Nat Commun **5:** 3425
1008 **Weits DA, Kunkowska AB, Kamps NCW, Portz KMS, Packbier NK, Nemec Venza Z,**
1009 **Gaillochet C, Lohmann JU, Pedersen O, van Dongen JT, Licausi F** (2019) An apical
1010 hypoxic niche sets the pace of shoot meristem activity. Nature **569:** 714-717
1011 **Weits DA, van Dongen JT, Licausi F** (2021) Molecular oxygen as a signaling component in
1012 plant development. New Phytol **229:** 24-35
1013 **White MD, Dalle Carbonare L, Lavilla Puerta M, Iacopino S, Edwards M, Dunne K, Pires E,**
1014 **Levy C, McDonough MA, Licausi F, Flashman E** (2020) Structures of Arabidopsis
1015 thaliana oxygen-sensing plant cysteine oxidases 4 and 5 enable targeted
1016 manipulation of their activity. Proc Natl Acad Sci U S A **117:** 23140-23147
1017 **White MD, Klecker M, Hopkinson RJ, Weits DA, Mueller C, Naumann C, O'Neill R, Wickens**
1018 **J, Yang J, Brooks-Bartlett JC, Garman EF, Grossmann TN, Dissmeyer N, Flashman E**
1019 (2017) Plant cysteine oxidases are dioxygenases that directly enable arginyl
1020 transferase-catalysed arginylation of N-end rule targets. Nat Commun **8:** 14690
1021 **Winkelmuller TM, Entila F, Anver S, Piasecka A, Song B, Dahms E, Sakakibara H, Gan X,**
1022 **Kulak K, Sawikowska A, Krajewski P, Tsiantis M, Garrido-Oter R, Fukushima K,**
1023 **Schulze-Lefert P, Laurent S, Bednarek P, Tsuda K** (2021) Gene expression evolution
1024 in pattern-triggered immunity within Arabidopsis thaliana and across Brassicaceae
1025 species. Plant Cell **33:** 1863-1887
1026 **Zhang H, Gannon L, Hassall KL, Deery MJ, Gibbs DJ, Holdsworth MJ, van der Hoorn RAL,**
1027 **Lilley KS, Theodoulou FL** (2018) N-terminomics reveals control of Arabidopsis seed

1028 storage proteins and proteases by the Arg/N-end rule pathway. New Phytol **218:**
1029 1106-1126
1030 **Zhang H, Sonnewald U** (2017) Differences and commonalities of plant responses to single
1031 and combined stresses. Plant J **90:** 839-855
1032 **Zhao Y, Wei T, Yin KQ, Chen Z, Gu H, Qu LJ, Qin G** (2012) Arabidopsis RAP2.2 plays an
1033 important role in plant resistance to Botrytis cinerea and ethylene responses. New
1034 Phytol **195:** 450-460
1035 **Zipfel C, Robatzek S, Navarro L, Oakeley EJ, Jones JD, Felix G, Boller T** (2004) Bacterial
1036 disease resistance in Arabidopsis through flagellin perception. Nature **428:** 764-767
1037 **Zou Y, Wang S, Zhou Y, Bai J, Huang G, Liu X, Zhang Y, Tang D, Lu D** (2018) Transcriptional
1038 Regulation of the Immune Receptor FLS2 Controls the Ontogeny of Plant Innate
1039 Immunity. Plant Cell **30:** 2779-2794
1040 **Zubrycka A, Dambire C, Dalle Carbonare L, Sharma G, Boeckx T, Swarup K, Sturrock CJ,**
1041 **Atkinson BS, Swarup R, Corbineau F, Oldham NJ, Holdsworth MJ** (2023) ERFVII
1042 action and modulation through oxygen-sensing in Arabidopsis thaliana. Nat Commun
1043 **14:** 4665
1044
1045
1046
1047
1048